Cloud-radiative effects on implied oceanic energy transports as simulated by atmospheric general circulation models

P.J. Gleckler[1], D.A. Randall[2], G. Boer[3], R. Colman[4], M. Dix[5], V. Galin[6],
M. Helfand[7], J. Kiehl[8], A. Kitoh[9], W. Lau[10], X.-Y. Liang[11], V. Lykossov[6],
B. McAvaney[4], K. Miyakoda[12], S. Planton[13], and W. Stern[12]

Abstract. This paper summarizes the ocean surface net energy flux simulated by fifteen atmospheric general circulation models constrained by realistically-varying sea surface temperatures and sea ice as part of the Atmospheric Model Intercomparison Project. In general, the simulated energy fluxes are within the very large observational uncertainties. However, the annual mean oceanic meridional heat transport that would be required to balance the simulated surface fluxes is shown to be critically sensitive to the radiative effects of clouds, to the extent that even the sign of the Southern Hemisphere ocean heat transport can be affected by the errors in simulated cloud-radiation interactions. It is suggested that improved treatment of cloud radiative effects should help in the development of coupled atmosphere-ocean general circulation models.

Introduction

The focus of this study is on the surface energy fluxes over the oceans simulated by current atmospheric general circulation models (AGCMs), and the implied oceanic meridional energy transports. We summarize the implied partitioning of meridional energy transport between the ocean and the atmosphere and compare them with available observations. The implied oceanic meridional energy transport varies dramatically from model to model, and we show that these differences are largely due to cloud-radiative effects. This result has important implications for coupled atmosphere-ocean general circulation models.

Uncoupled AGCM simulations are performed by prescribing sea-surface temperatures (SSTs) and sea ice distributions. In a similar way, uncoupled ocean general circulation models (OGCMs) are integrated with prescribed surface wind stresses and relaxation of surface temperatures and salinity toward prescribed climatological values. Simulations produced by these models are quite realistic, but they are strongly constrained by the prescribed boundary conditions. Climate change studies must account for interactions between the ocean and the atmosphere, and so efforts are underway to couple AGCMs and OGCMs. When the boundary constraints are removed, in the coupled models, the simulated climate typically "drifts" towards an unrealistic state. To prevent this, most coupled models use "flux corrections," including ad hoc adjustments to the surface energy flux distribution (Manabe and Stouffer, 1993). We need to

[1]Program for Climate Model Diagnosis and Intercomparison, Livermore
[2]Colorado State University, Fort Collins, Colorado
[3]Canadian Climate Centre, Victoria
[4]Bureau of Meteorology Research Centre, Melbourne
[5]Commonwealth Scientific and Industrial Research Organization, Mordialloc
[6]Department of Numerical Mathematics, Moscow
[7]Goddard Space Flight Center, Greenbelt
[8]National Center for Atmospheric Research, Boulder
[9]Meteorological Research Institute, Tsukuba
[10]Goddard Laboratory for Atmospheres, Greenbelt
[11]State University of New York, Albany
[12]Geophysical Fluid Dynamics Laboratory, Dynamic Extended Range Forecasting, Princeton
[13]Centre National de Recherches Meteorologiques, Toulouse

understand why such corrections are needed, so that ultimately they may be minimized or altogether eliminated. The results of this study shed light on this issue.

The need for a systematic and comprehensive intercomparison of AGCMs has been recognized by the World Climate Research Programme for some time. The Atmospheric Model Intercomparison Project (AMIP) (Gates, 1992) is the most recent such endeavor. AMIP simulations are 10 years long, and participating models use boundary conditions based on satellite-derived estimates of monthly mean SSTs and sea ice distributions for 1979-1988. Here we report on findings from AMIP subproject No. 5, using results from 15 AMIP AGCMs. All model results are ten year averages.

We must emphasize that when AGCMs are run with specified SSTs and sea ice, as in the AMIP runs, the surface radiation fluxes over the oceans are largely immaterial to the simulated atmospheric circulation. In particular, the simulated atmospheric circulation can be very realistic even if the surface radiation fluxes are not realistic. It is only when the AGCM is used as the atmospheric component of a coupled atmosphere-ocean model that the surface radiation fluxes become critical for the simulated climate.

Background

Annual-mean meridional energy transport can be defined for the atmosphere, T_A, the ocean, T_O, and the combined ocean-atmosphere system, T_{A+O}. Defining ϕ as latitude and a as the radius of the earth, the annual-average energy equations for the atmosphere, the ocean and the combined system are (see Fig. 1):

$$\frac{1}{a \cos \varphi} \frac{\partial}{\partial \varphi} F_A \cos \phi = R_{top} - R_{ocn} - LH - SH$$
$$= R_{top} - N_{ocn},$$

(1.a)

$$\frac{1}{a \cos \varphi \partial \varphi} F_O \cos \phi = + R_{ocn} + LH + SH = N_{ocn},$$

(1.b)

$$\frac{1}{a \cos \varphi \partial \varphi} F_{A+O} \cos \phi = R_{top},$$

(1.c)

respectively, where the F's represent northward energy fluxes. The vertical fluxes (downward being positive) R_{top}, R_{ocn}, LH and SH represent the zonal mean (average along a circle of constant latitude) "top-of-the-atmosphere" net radiative flux, and the ocean surface net radiative, latent and sensible heat fluxes respectively. The net ocean surface energy flux is $N_{ocn} = R_{ocn} + LH + SH$. A similar equation could be written for the land but, because there is essentially no horizontal energy transport through the land, that equation is not needed here and the zonal averages of the surface fluxes in Eqs. 1.a-1.c are computed using ocean values only.

The horizontal transport of energy across a latitude circle is $T = 2\pi a \cos \phi F$, so that the equations above take the general form

$$\frac{1}{2\pi a^2} \frac{\partial}{\partial \phi} \left(T_{A+O}, T_A, T_O \right) =$$
$$\left(R_{top}, R_{top} - N_{ocn}, N_{ocn} \right) \cos \phi.$$

(2)

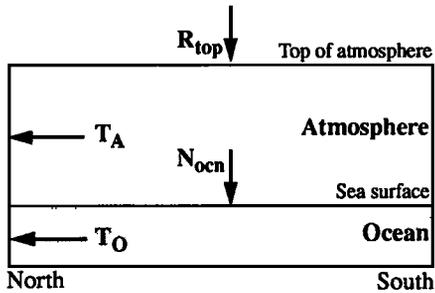The northward transport may then be inferred from

Figure 1. Schematic of energy flows in the atmosphere-ocean system. Northward meridional energy transports are defined as positive, as are downward vertical fluxes.

$$\left(T_{A+O}, T_A, T_O\right)(\phi) =$$

$$2\pi a^2 \int_{-\pi/2}^{\phi} \left(R_{top}, R_{top} - N_{ocn}, N_{ocn}\right) \cos \phi' \, d\phi' \qquad (3)$$

for the total system and also for the atmosphere and the ocean separately, provided that the appropriate fluxes are known. The transports may also be obtained directly from observations of the atmosphere and the oceans. For example, Eq. 4 illustrates how atmospheric transports can be evaluated using measurements of temperature, geopotential, moisture and winds (Oort, 1983):

$$T_A(\phi) = 2\pi a \cos \phi \int_{surface}^{top} \overline{\left[(c_p t + gz + Lq)v\right]} dz \ . \qquad (4)$$

Here c_p is the specific heat capacity of dry air, t the air temperature, g the accleration due to the Earth's gravity, z the height, L the latent heat of vaporization, q the specific humidity and v the meridional wind. The brackets represent a zonal average, and the overbar an average in time. A similar equation can be written for ocean energy transport. Direct oceanic estimates are more difficult because of the lack of data on the three-dimensional distributions of oceanic temperatures and currents, but have been made at a few latitudes (Bryden et al., 1991).

The AMIP integrations are performed using atmospheric general circulation models with prescribed SSTs and sea ice distributions. The AGCMs simulate surface and top-of-the-atmosphere fluxes given these boundary conditions and the simulated working of the atmosphere, but the SSTs and sea ice do not respond to the local surface fluxes since there is no explicit oceanic adjustment. Although no explicit oceanic meridional energy transport is computed by the models, we use the oceanic energy transports implied by the simulated ocean surface fluxes (Eq. 3). Alternatively, calculating T_A from the appropriate top-of-the-atmosphere and surface fluxes allows one to calculate T_O by subtraction $(T_O = T_{A+O} - T_A)$. Note that the implied oceanic transports obtained by this method will be in error if the long term net energy flux over land is not exactly zero, or if there is energy accumulating in the atmosphere or ocean. In our calculations, any non-zero annual mean of the globally averaged boundary fluxes (the right hand side of Eqs. 1a-1c) is removed uniformly over the globe. The imbalances in the AMIP simulations range between -10 and 10 Wm^{-2}. Tests have demonstrated that the assumed geographical distribution of the globally averaged energy imbalance does not alter the conclusions presented in this paper.

Results

Fig. 2a shows T_{A+O} as inferred from Eq. 3 using 4 years of net top-of-the-atmosphere radiation as observed in the Earth Radiation Budget Experiment (ERBE) (Barkstrom et al., 1990), and as simulated by the models. There is a broad range of simulated transports in Fig. 2a (especially in the Southern Hemisphere), which are generally less than observed. T_{A+O} is known with more accuracy than T_A or T_O because it is based on more reliable observations.

Fig. 2b shows observationally derived annual mean estimates of T_A by Oort (1983), Trenberth and Solomon (1994), and
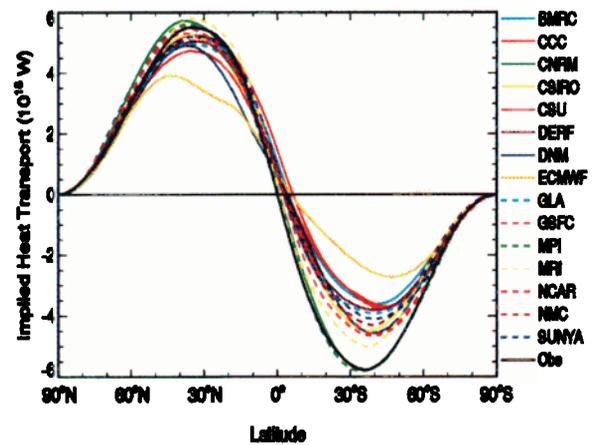

Figure 2a. Annual mean total northward meridional energy transport: implied by simulations and observations.
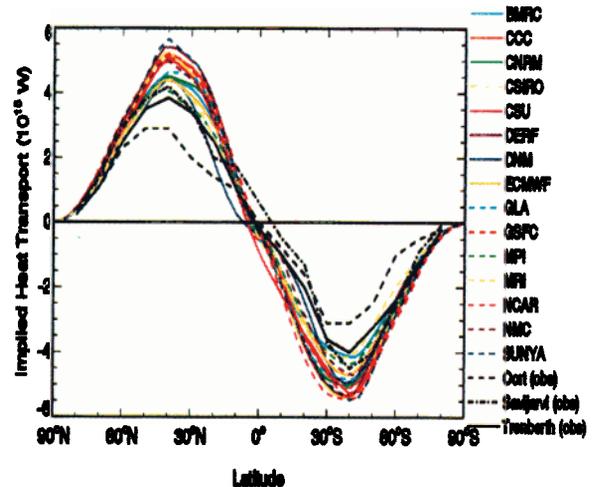

Figure 2b. Annual mean northward atmospheric meridional energy transport: as simulated and observed.
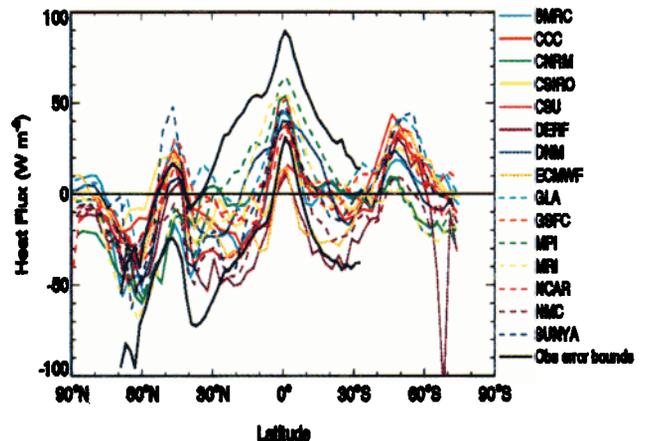

Figure 2c. Zonal and annual average net ocean surface heat flux: observational error bounds and simulated.

Savijarvi (1988) obtained from meteorological observations, as well as the T_A results produced by the models. Trenberth used operational weather prediction analyses produced by the European Centre for Medium Range Weather Forecasts, while Savijarvi and Oort both used the same gridded radiosonde data. Savijarvi modified the radiosonde wind data to satisfy a dynamical constraint based on vorticity balance, whereas Oort did not. As shown in Fig. 2b, the results of Trenberth and Savijarvi agree very well in the Northern Hemisphere mid-latitudes where observations are best, even though they are based on independent data sources and analysis methods. They also agree reasonably well with the model simulations. The T_A estimate by Oort, on the other hand, is considerably smaller than the other observational estimates and the model results.
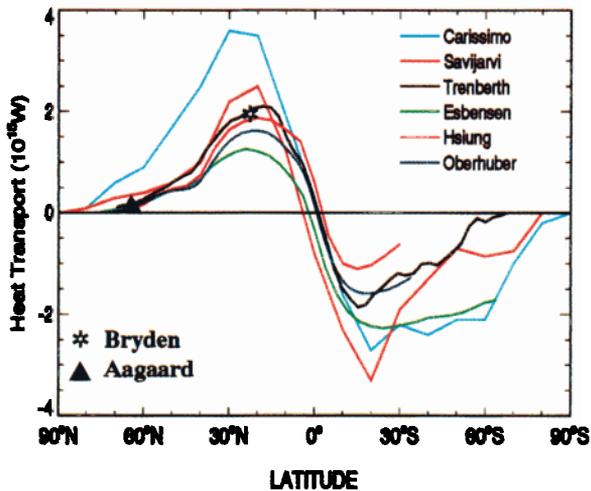
Figure 3a. Annual mean global ocean northward meridional energy transport: observational estimates.
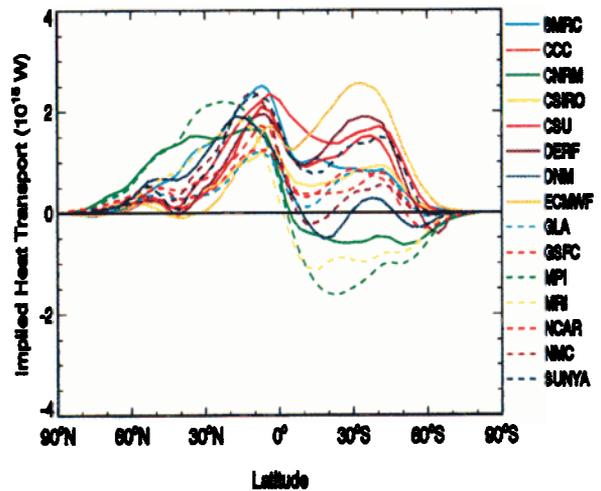

Figure 3b. Annual mean global northward oceanic meridional energy transport: implied by simulations.
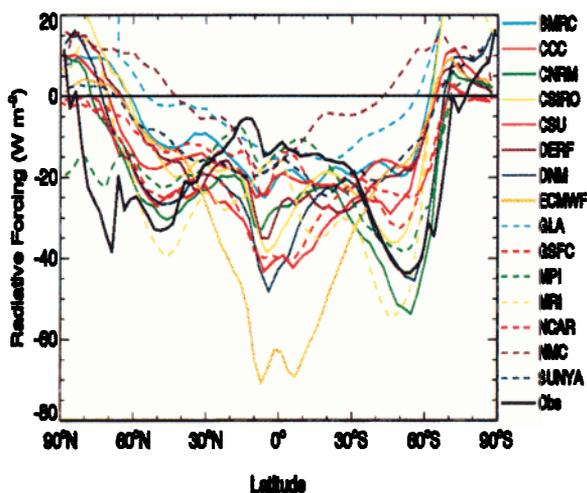

Figure 3c. Zonal and annual average net top of the atmosphere cloud radiative forcing: observations and simulations.
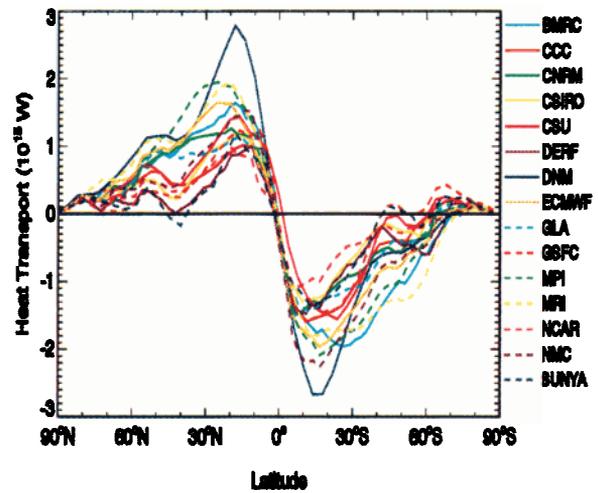

Figure 3d. Zonal and annual average net cloud radiative forcing: as simulated and observed. Annual average "hybrid" global ocean northward meridional energy transport: T_{A+O} (observed) - T_A simulated).

Figure 2c shows the zonally averaged annual mean net ocean surface energy flux, N_{ocn}, simulated in the available AMIP runs. Observationally based error bars (Gleckler, 1993) are also shown. At most latitudes, the simulated N_{ocn} is within the error bars, although some of the models produce too little tropical net surface heating. For some of the models N_{ocn} is greater at 50° S than it is in the tropics. Although this may seem a priori implausible, we cannot rule it out as a possibility because of the great uncertainties in the Southern Hemisphere data and the complexities of the surface energy balance.

T_O may be inferred from the observational estimates of Nocn, and computed as a residual, using $T_O = T_{A+O} - T_A$, where T_{A+O} and T_A are the observations shown in Figs. 2a and 2b. T_O can also be directly derived from east-west hydrographic transects which span all ocean basins at the same latitude (Bryden et al., 1991). Fig. 3a depicts observationally based estimates of T_O from eight sources. Three are based on the residual method. The curve labeled "Savijarvi" is obtained by subtracting Savijarvi's T_A estimate from the ERBE-based T_{A+O}. Carissimo et al. (1985) used Oort's T_A. Carissimo's estimate of T_O was made before the ERBE data were available, but the satellite data he used yielded an implied T_{A+O} which differs little from that of ERBE. The third estimate of T_O was made by Trenberth and Solomon(1994), using his T_A estimate and the T_{A+O} implied by ERBE. An important distinction between Trenberth's estimate and that of Savijarvi and Carissimo is that Trenberth utilized several additional physical constraints, most notably adjusting the implied T_O by correcting for spurious non-zero long-term net land-surface heating implied by the data. Three of the curves in Fig. 3a are inferred (from Eq. 3) using the climatological N_{ocn} data of Oberhuber (1988), Esbensen and Kushnir (1981) and Hsiung (1985), respectively. Although these curves are qualitatively similar, they are not considered to be highly reliable (Tally, 1985). Two direct

estimates of T_O, based on hydrographic transects (Bryden et al, 1991, and Aagaard and Greisman, 1975) are also shown in Fig. 3a. The direct estimates are believed to be fairly accurate, especially the estimate for 65° N. Despite the general qualitative agreement seen in Fig. 3a, Southern Hemisphere data deficiencies are so severe that we cannot even be sure of sign of T_O.

Fig.3b shows the implied T_O obtained from N_{ocn} fluxes of the AMIP simulations. For the Northern Hemisphere the AGCMs are in general qualitative agreement with the observations shown in Fig. 3a except for those of Carissimo et al. Although there is a large spread of results among the models, many have a maximum northward (poleward) Northern Hemisphere transport of $T_O \sim 2$ x10^{15} W. The latitude at which this maximum occurs varies considerably from model to model. For the Southern Hemisphere, the range in the models' implied T_O is much larger; the implied T_O is northward (equatorward) in many cases, and southward (poleward) in only a few. The strong downward N_{ocn} at 50° S in some of the models (see Fig. 2c), tends to force northward ocean transport between 50° S and the Equator.

It is important to identify the causes of these large discrepancies between the observed and simulated surface fluxes and implied ocean transports in the Southern Hemisphere. AGCMs are known to disagree considerably in their simulations of the effects of clouds on the Earth's radiation budget (Cess et al., 1990), and hence the effects of simulated cloud-radiation interactions on the implied meridional energy transports are immediately suspect. Unfortunately, we do not have global data on the effects on clouds on the surface energy budget, either as simulated by the models or from observations. We do, however, have observations of the effects of clouds on R_{top} and thus T_{A+O}.

The cloud radiative forcing (CRF) is defined (Ramanathan et

al., 1989) as the difference between the net radiation at the top of the atmosphere with the given distribution of cloudiness, and R_{clr}, which we define to be the net radiation at the top of the atmosphere which would have been observed if no clouds were present but all else (e.g. temperature and water vapor) remained the same. Thus $CRF \equiv R_{top} - R_{clr}$. Clouds influence atmospheric heating primarily by trapping longwave energy within and beneath the cloud layer, and by reflecting sunlight back to space. Fig. 3c shows the zonally and annually averaged CRF from both the simulations and the ERBE data. There are large differences among the CRF simulated by the various models, and for the most part also between the observed and simulated cloud radiative forcing. In comparison with the ERBE data, many of the models underestimate the magnitude of the CRF at mid-latitudes but overestimate it in the tropics. Poleward of 60° in both hemispheres the CRF observations are not reliable. The underestimate of the CRF in the Southern Hemisphere mid-latitudes is especially important for the implied T_O because the Southern Hemisphere oceans are much more extensive than those of Northern Hemisphere. A close comparison of these results and those in Fig. 2c suggests that there is a strong correlation between the magnitudes of the CRF and N_{ocn}, and that differences in T_{A+O} and T_O are linked and largely due to cloud effects in the models. The discrepancies between the simulated and observed $CRFs$ suggest that the simulated implied northward T_O in the Southern Hemisphere is erroneous and is due to inadequate simulations of the CRF.

We may connect the implied oceanic transport to the cloud radiative forcing using Eqs. 1-3. In particular, it follows from Eq. 3 that:

$$T_{A+O} = 2\pi a^2 \int_{-\pi/2}^{\phi} \left\{ R_{clr} + \left(R_{top} - R_{clr} \right) \right\} \cos \phi d\phi \qquad (5.a)$$

$$= 2\pi a^2 \int_{-\pi/2}^{\phi} \left\{ R_{clr} + CRF \right\} \cos \phi d\phi \qquad (5.b)$$

$$= T_{clr} + T_{CRF} , \qquad (5.c)$$

where T_{clr} represents the T_{A+O} inferred from a "clear-sky" atmosphere, and T_{CRF} is that due to the radiative effects of clouds. We have computed a "hybrid" T_O defined by:

$$\bar{T}_O \equiv T_{A+O}^{ERBE} - T_A \qquad (6.a)$$

$$= \left(T_{A+O} - T_A \right) + \left(T_{A+O}^{ERBE} - T_{A+O} \right) \qquad (6.b)$$

$$= T_O + \delta T_{clr} + \delta T_{CRF} \qquad (6.c)$$

Here is the T_{A+O}^{ERBE} inferred from the ERBE data. The δT_{clr} and δT_{CRF} represent the difference between the observed and simulated T_{A+O} resulting from the effects of clouds and a clear-sky atmosphere respectively. Comparison of the simulated cloudy and clear-sky fluxes has demonstrated that we can neglect the clear-sky effects on the implied T_O and thus:

$$\bar{T}_O \cong T_O + \delta T_{CRF} . \qquad (7)$$

The resulting hybrid T_O, which is based partly on observations and partly on simulations, is shown in Fig. 3d. The contrast with Fig. 3b is remarkable; in Fig. 3d, all of the hybrid results show poleward T_O in both hemispheres as a consequence of the cloud forcing "corrections."

Conclusions

The AGCMs shown here were run with fixed SSTs. The ocean energy transports inferred from these runs are not necessarily the same as the ocean energy transports that would be produced in coupled ocean-atmosphere simulations with the same AGCMs. Nevertheless, our results show that prescribed realistic SST distributions lead current AGCMs to produce surface energy

budgets (Fig. 2c) that imply ocean energy transports that vary widely from model to model (Fig. 3b), especially in the Southern Hemisphere. These implied ocean energy transports cannot all be right, although they can all be wrong. Observations of the surface energy budget and/or the ocean circulation are not adequate to say which of the AGCM-implied ocean energy transports, if any, is correct. It is difficult to believe however, that the ocean energy transports could be equatorward at all latitudes in the Southern Hemisphere.

This paper presents quantitative evidence that the model-to-model variations in the implied ocean energy transports are largely due to model-to-model differences in the simulated cloud radiative forcing, which is a comparatively well observed quantity except at high latitudes. Our results thus indicate that as future AGCMs produce more realistic cloud radiative forcing, the simulated surface energy budget should improve. Coupled-model simulations without flux corrections should also improve, although other factors are important such as the simulation of the surface fresh water flux and wind stress.

References

Aagaard, K. and P. Greisman, Toward new mass and heat budgets for the arctic ocean, *J. Geophys. Res., 80,* 3821, 1975.

Barkstrom, B., H. Harrison, and R. Lee, The earth radiation budget experiment, *EOS, 71, No. 9,* 297, 1990.

Bryden, H. L., D.H. Roemmich, and J.A. Church, Heat transport by ocean currents across 24°N, *Deep-Sea Res., 38,* 297, 1991.

Carissimo, B.C., A.H. Oort, and T.H. Vonder Haar, Estimating the meridional energy transports in the atmosphere and ocean, *J. Phys. Oceanogr., 15,* 82, 1985.

Cess, R.D., et al, Intercomparison and interpretation of climate feedback processes in 19 atmospheric general circulation models., *J. Geophys. Res., 95,* 16,601, 1990.

Esbensen, S.K. and Y. Kushnir, The heat budget of the global ocean, *Report No. 29,* Oregon State University, Climatic Research Institute, 1981.

Hsiung, J., Estimates of global oceanic meridional heat transport, *J. Phys. Oceanogr., 15,* 1405-1413, 1985.

Gates, W.L., The Atmospheric Model Intercomparison Project, *Bull. Amer. Met. Soc. 73,* 1962, 1992.

Gleckler, P.J., The partitioning of meridional energy transport between the ocean and the atmosphere, Ph.D. dissertation, University of California at Davis (1993).

Manabe, S. and R. J. Stouffer, Century-scale effects of increased atmospheric CO_2 on the ocean atmosphere system, *Nature,* 364, 216, 1993.

Oberhuber, J. M., Report No. 15, The budgets of heat, buoyancy and turbulent kinetic energy at the surface of the global ocean, Max Planck Institute for Meteorology/Hamburg, 1988.

Oort, A. H., Global atmospheric circulation statistics, 1958-1973, *Prof. Pap. No. 14,* National Oceanographic and Atmospheric Administration, 1983.

Ramanathan, V., et al., Cloud-radiative forcing and climate: results from the Earth radiation budget experiment, *Science,* 243, 57, 1989

Savijarvi, H. I., Global energy and moisture budgets from rawinsonde data, *Mon. Wea. Rev., 116,* 417, 1988.

Talley, L. D., Meridional heat transport in the Pacific Ocean, *J. Phys. Oceanogr., 14,* 213 1985.

Trenberth, K. and A. Solomon, The global heat balance: heat trasports in the atmosphere and ocean, *Clim. Dyn., 10,* pp. 107-134, 1994.

P.J. Gleckler, Program for Climate Model Diagnosis and Intercomparison, Lawrence Livermore National Laboratory, Livermore, CA, 94551. (e-mail: gleckler@airsea.llnl.gov)

D.A. Randall, Department of Atmospheric Science, Colorado State University, Fort Collins, CO. (e-mail: randall@redfish.colostate.edu)